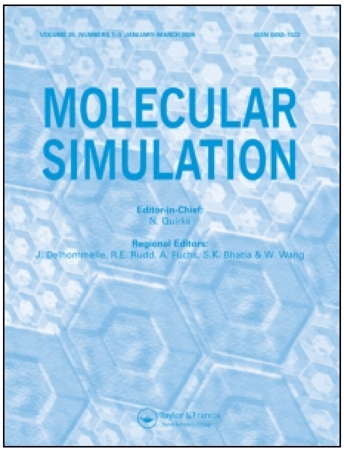

Molecular Simulation
Publication details, including instructions for authors and subscription information:
http://www.informaworld.com/smpp/title~content=t713644482

Molecular simulation study on sorption and diffusion processes in polymeric pervaporation membrane materials

C. Schepers[a]; D. Hofmann[a]
[a] Institute of Chemistry, GKSS Research Centre Geesthacht, tow, Germany

To cite this Article Schepers, C. and Hofmann, D.(2006) 'Molecular simulation study on sorption and diffusion processes in polymeric pervaporation membrane materials', Molecular Simulation, 32: 2, 73 — 83
To link to this Article: DOI: 10.1080/08927020500474292
URL: http://dx.doi.org/10.1080/08927020500474292

Molecular Simulation, Vol. 32, No. 2, 15 February 2006, 73–83

Taylor & Francis
Taylor & Francis Group

Molecular simulation study on sorption and diffusion processes in polymeric pervaporation membrane materials

C. SCHEPERS and D. HOFMANN*

Institute of Chemistry, GKSS Research Centre Geesthacht, Kantstr. 55, D-14513 Teltow, Germany

(Received September 2006; in final form November 2006)

Since MD simulations of membrane separation processes of aqueous/organic solutions lead to reasonable results that are in good agreement with experimental investigations an approach has been made to apply this method also for organic/organic membrane separation. In this connection the separation of a model feed mixture of 20 wt% benzene and 80 wt% *n*-heptane with dense amorphous polymer membranes was simulated utilising molecular modelling techniques. Special modifications of standard polymers such as polymethacrylates and polysiloxanes were investigated. It could be demonstrated that MD simulations of polymer–feed interface models can reproduce at least qualitatively important experimental results from related membrane pervaporation processes. These models are therefore suited in principle to obtain a better insight in the atomistic mechanisms of pervaporation. In addition, the knowledge about the underlying diffusion mechanism could be improved.

Keywords: Polymeric membranes; Pervaporation; Molecular dynamics simulations; CAMM

1. Introduction

During the last 15 years atomistic computer aided molecular modelling (CAMM) has become a widely used method for the investigation of the molecular structure of amorphous polymers and the diffusion and solubility of small molecules through these materials (cf. e.g. feature articles [1,2]). The applied methodology of molecular dynamics (MD) simulations is based on the principles of classical mechanics and does, thus enable the handling of much larger models than quantum chemistry. Many of these simulations dealt with gas diffusion in the bulk of different rubbery and glassy polymers. In addition, there are only few papers on MD simulations in which the separation behaviour of a pervaporation membrane is described, also mainly considering the polymer bulk [3–5]. It could be demonstrated that in general currently available advanced MD simulations techniques and force-fields are capable of at least qualitatively reproducing initial sorption processes at the interfacial region of polymer and solvent.

It is the main aim of this paper to describe applications of CAMM investigations which in the future may help to solve this problem for the relevant example of benzene/*n*-heptane mixtures by better understanding the underlying pervaporation mechanism on an atomistic scale, which are not available by any experimental method, and predictions of separation trends.

2. Methods

Pervaporation is an important energy saving separation technology for the separation of liquid mixtures. There, a membrane separates a liquid feed mixture (upstream side) from a vapour phase (permeate on the downstream side), while the transport occurs in the direction of the vapour. During the separation process a phase transition occurs inside the membrane. Polymeric pervaporation membranes have hitherto mainly been used to separate (near) azeotropic mixtures of low molecular weight liquids where in most cases one component was water.

The separation of mixtures of water and organic molecules like ethanol and methanol using pervaporation membranes is technically widely solved. In those cases also predictions made by MD simulations were found to be in good agreement with the experimental results [2]. But there is still no successful large-scale commercial solution known for the pervaporation of organic/organic (like aromatic/aliphatic) liquid mixtures. This in part has to do with the fact that although major aspects of the discussed separation mechanism are determined by the static structure and the

---

*Corresponding author. Tel.: +49-3328-352247. Fax: +49-3328-352452. Email: hofmann@gkss.de

Molecular Simulation
ISSN 0892-7022 print/ISSN 1029-0435 online
http://www.tandf.co.uk/journals
DOI: 10.1080/08927020500474292

dynamic behaviour of the separation system (membrane plus penetrants) on a molecular scale, it is impossible to get sufficient direct experimental information about what is happening in these dimensions during pervaporation. Although a lot of research on pervaporation processes has been published [6–10], there is still more information needed to understand the sorption–diffusion mechanisms on the molecular level. This knowledge is particularly important for the development of membrane polymers for the pervaporation separation of organic/organic mixtures. Therefore a better basic comprehension, e.g. by MD simulations is clearly wanted.

The underlying separation mechanism is of the sorption–diffusion type [11]: First the molecules of the feed phase have to be selectively sorbed into the membrane at the upstream side, second diffusion through the membrane takes place and third the permeants get desorbed into the vapour phase at the downstream side. There the solution of a penetrant molecule species A in the membrane is described with the solubility parameter S_A (e.g. in g (penetrant)/cm^3 (polymer)), while the solubility of species B of a binary mixture is S_B. The selectivity of a membrane, on the other hand, is often characterised by the separation factor α [6]:

$$\alpha_{\mathrm{A/B}}\,\frac{(c_A/c_\mathrm{B})_\mathrm{permeate}}{(c_\mathrm{A}/c_\mathrm{B})_\mathrm{feed}} \tag{1}$$

with c_A and c_B being the concentrations of components A and B in the respective phase. According to Fick's first law the diffusivity of the permeants is characterised with the constants of diffusion D_A (in cm^2/s) and D_B, respectively. The fact that in pervaporation processes besides the permeate pressure the sorptive stage at the upstream side of the membrane is often very decisive particularly for the achievable separation factors, has led the authors of the current study to an extended approach towards pervaporation systems employing interface models for the upstream polymer–feed region [12–14]. In these papers, results for the pervaporation of aqueous solutions of ethanol through polysiloxane and polyvinylalcohol (PVA) were reported.

With regard to the applied MD simulation concepts it should be stressed that there only the initial stages of adsorption, absorption and diffusion near the membrane-feed interface region could be investigated, while the remarks made above on the sorption–diffusion mechanism considered macroscopic samples where, e.g. Fick's law describes a statistical transport process.

3. Materials and simulation details

This paper presents results of new MD simulations of interface phenomena during pervaporation processes for the example of an organic/organic feed mixture. As model system for such a binary organic mixture with close boiling points a solution of 20 wt% benzene in 80 wt% *n*-heptane was chosen. Since, hitherto no polymeric material is known that would e.g. meet the desired selectivity $\alpha_{\mathrm{benzene}/n\text{-}\mathrm{heptane}}$ of at least 10, a number of materials suggested by experimentalists [15] were subjected to respective MD simulations. The discussed results concern for instance trend predictions for the initial sorptive stage of the pervaporation at the polymer–feed interface and better insight in potential differences in the diffusion mechanisms for the conformationally rigid benzene and the conformationally rather flexible *n*-heptane penetrant molecules.

The investigated classes of polymers were polysiloxanes and polymethacrylates. Figure 1 contains all investigated structures. The polysiloxanes poly(dimethyl siloxane) (PDMS) and poly(methyl phenyl siloxane) (PMPhS) were included on the one hand for comparison with the mentioned foregoing successful simulations on the pervaporation of water–ethanol mixtures through these materials. On the other hand, the effect of substituting one methyl group in PDMS by a benzene ring in PMPhS was of interest. In the latter highly flexible polymer, the "like dissolves in like" principle should be valid. Thus, the solubility for benzene should increase in comparison to PDMS.

Due to the possibility that carboxylic (COOR) groups of polymethacrylates may serve as electrophilic targets for approaching benzene molecules, polymers containing these groups were considered by experimentalists to be promising candidates for the solution of the mentioned separation problem [15]. It was for instance known that the presence of such groups in polymers can improve the benzene selectivity in the case of benzene/cyclohexane feeds [16,17].

In addition, most of the considered modifications (PBMA, PNMA, PAMA, PtBMA and PMPhSMA) of PMMA contained aromatic rings. The series PBMA, PNMA and PAMA more specifically shows an increasing contents of aromatic sub-structures. Following the "like dissolves in like" principle which was found for low molecular weight liquid systems was to be tested whether these functional groups can enhance the benzene solubility compared with PMMA.

Another approach represents PMPhSMA, that contains electron accepting silicon-atoms which may undergo energetically favourable interactions with the π-electrons of benzene, a π-electron donor. In addition there are reports in the literature that silicone-modifications of polymers can lead to improved benzene solubilities [18].

In order to improve the diffusivity of the preferentially sorbed permeand a third aspect was to increase the free volume (space not being occupied by polymer atoms) in the polymer. Therefore PtBMA was considered which is expected to have a relatively high amount of free volume due to its bulky substituents.

It should be mentioned that all the described modification ideas were based either on the "like dissolves in like" principle or on quantum chemical predictions for small molecules. In polymers, however, the distribution and dynamics of the free volume are also very important, which means that the relatively simple design rules used might be overlaid by other effects, e.g. due to

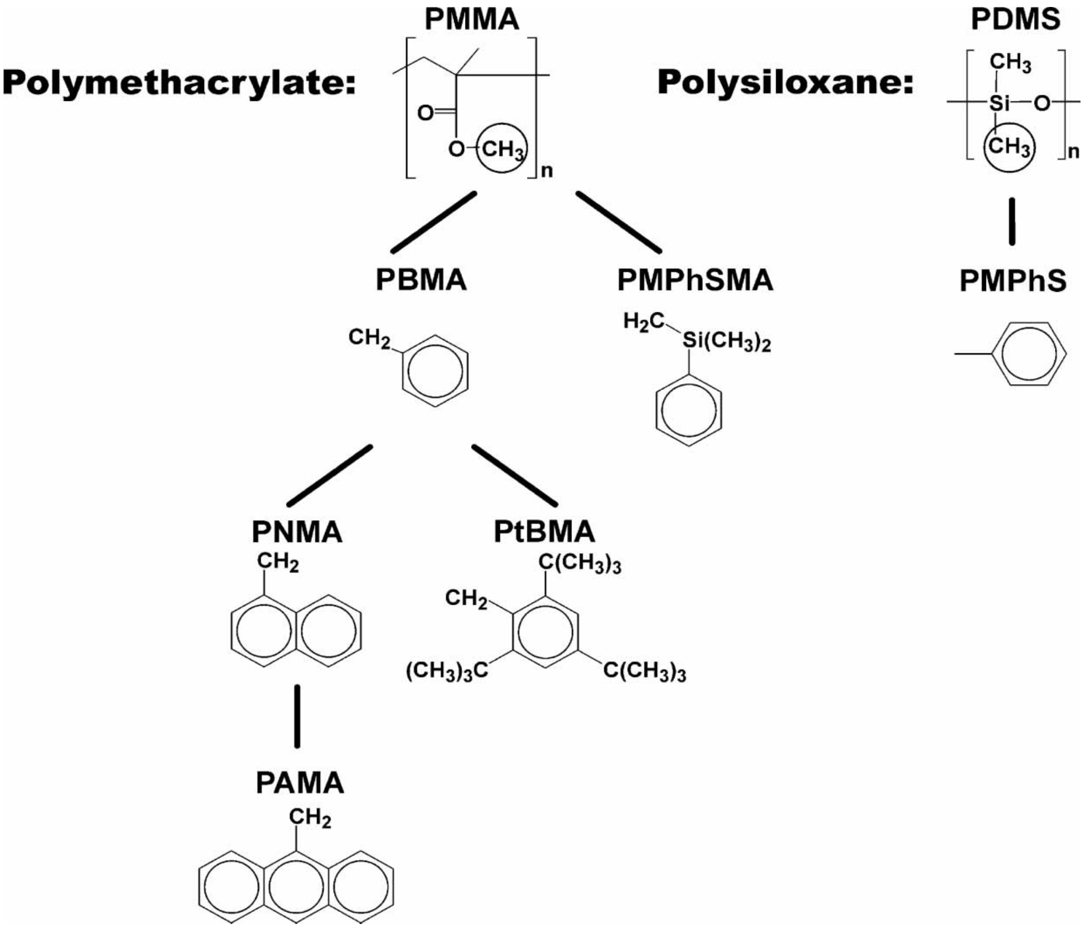

Figure 1. Selection scheme for the simulated polymers.

arrangements of secondary structures. Here atomistic molecular modelling based on force-fields and Newton's equations can help to estimate whether the application of the mentioned concepts may lead to improved materials.

The InsightII/Discover software of Accelrys (former Molecular Simulations) [19] was applied for the construction and the atomistic simulations. For the potential energy calculations the pcff force-field [20] was used. This choice was based on the positive experience made with pcff for polymer–feed interface models in the case of aqueous solutions [12–14].

The density of a polymer to be modelled is an important parameter for the algorithm used to fill the basic volume element of a model with the respective chain segments. Since related experimental reference data were only available for the polymers PDMS, PMPhS, PMMA and PBMA, the densities for the other model polymers were estimated using the Synthia module of the Accelrys InsightII software. Synthia is a quantitative structure property relations programme based on semi-empirical calculations, including different atom types and bond topology of the respective polymer [21,22]. As shown in table 1, Synthia seems to provide reasonable estimates for the polymers with available experimental density values. Therefore also the predicted data for the remaining polymers are considered appropriate for the model construction. Changes of physical properties like individual component densities and swelling that occur during the course of simulation MD are influenced by the respective force-field. Table 1 also contains predicted and measured data on the glass transition temperatures T_g of the polymers, which are in good agreement especially considering the measurement uncertainty.

The construction of the single phase bulk models of amorphous polymers is described in detail in reference [6]. Therefore, here only some peculiarities for creating interface models are described. The interface simulation models were composed of two sub-packing models in each case, one for the respective polymer and one for the respective feed mixture (figure 2).

Each pure polymer box and pure feed box was packed separately utilising the amorphous cell module of the InsightII software to obtain an initial guess filling with chain segments or feed molecules. The basic initial packing procedure follows the Theodorou–Suter algorithm [23,24]. This procedure normally assumes a three-dimensional (3D) translation symmetry. In the given case, however, the polymer-packing model is later to be combined with a two component liquid mixture to form the interface. The lateral (x,y) dimensions of the model

Table 1. Estimates of densities ρ_{Synthia} (plus where available measured values ρ_{exp}) and glass transition temperatures $T_{\mathrm{g,Synthia}}$.

System	*Simulation temperature T in K*	*Polymer density in g cm^{-3}*		*$T_{g,Synthia}$ in K*
		ρ_{exp} at 298 K	*$\rho_{Synthia}$ (T)*	
PDMS	303	0.95[†]	0,952	154
PMPhS	303	1.102[‡]	1,108	213
PMMA	303		1,157	355
PBMA	303	1.188[‡]	1,177	385
PNMA	303	–	1,186	406
PAMA	303	–	1,220	419
PtBMA	303	–	0,967	365
PMPhSMA	303	–	1,040	375
PMPhSMA	353	–	1,028	375

[†] Literature data taken from ref. [25]. [‡] Measured with the gradient tube method [26].

have to be fixed before the actual packing procedure to permit the later necessary combination with the respective other component (i.e. feed or polymer) of the interface model. In the third dimension penalty surface potentials (equation (1)) force the non-periodic (z) coordinates of the constituent atoms in a layer of a thickness that results from the other two box-lengths and the intended density of the system. The shape of this potential term leads to prohibitively high energy penalties for atoms i whose z_i-coordinates come close to the minimum ($z = 0$) or maximum ($z = z_{\mathrm{max}}$) z-coordinate of the basic volume element.

$$U_z = K_z \sum_i \left(\frac{1}{z_i^m} + \frac{1}{(z_i - z_{\mathrm{max}})^m} \right) \tag{2}$$

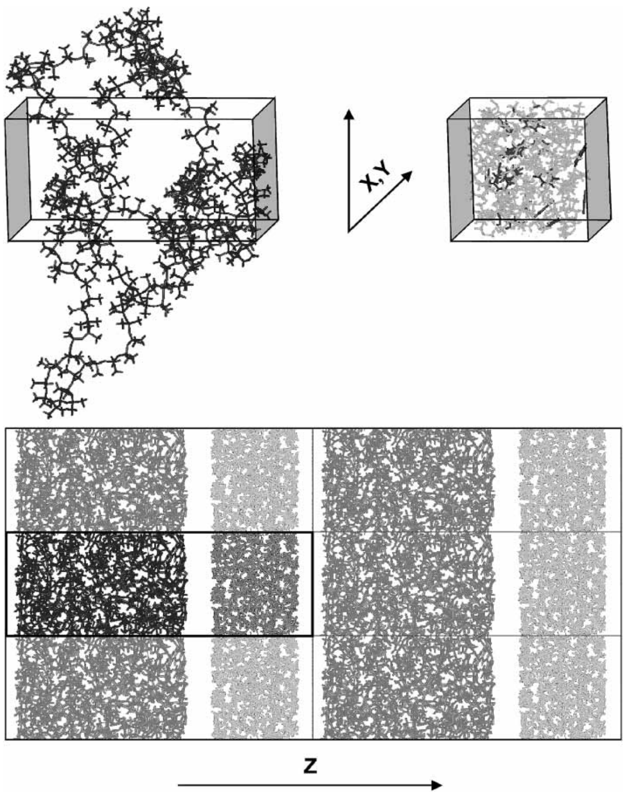

Figure 2. Construction of a 3-dimensional periodic (3D-PBC) interface model from a 2-dimensional periodic (2D-PBC) polymer packing model and a 2D PBC solvent packing model (Example PDMS and benzene/n-heptane).

m is an even integer of at least a value of 8. K_z is the chosen force constant which is normally selected by trial and error in a way to avoid any atom coming closer than about 1 Å to $z = 0$ or $z = z_{\mathrm{max}}$.

Due to the presence of aromatic and non-aromatic rings in most of the investigated polymer structures, unwanted catenation or spearing of those rings does often occur if the packing procedure is performed at the experimental density. In order to avoid those unwanted effects the following specific approach was used in each case. The initial packing was performed at very low densities of less than 0.1 g/cm^3. Because of the fixed dimensions of the packing model in the x- and y-directions the resulting initial packing models became very long (several 100 Å) in z-direction. Those models were then first equilibrated under *NVT* (constant atom number N, constant model volume V and constant simulation temperature T) conditions using sequences of static structure optimisation and MD simulations combined with force-field parameter scaling according to stages 1–5 of table 2.

In the subsequently necessary stages of model compression and further equilibration it had to be considered that due to the presence of penalty surface potentials the Discover software of Accelrys Inc. does not allow for reasonable pressure calculations. Therefore, in this case no *NPT* ($P =$ constant simulation pressure) simulations at high pressure could be utilised for the model compression towards the desired experimental density of the intermediate models. Instead, the stepwise compression of the model was performed as follows: First in equation (2) the strength parameter K_z was increased to a very high value of up to 10^6 kcal∗Å^m/mol. This potential pushed the polymer segments about 2 nm away from the bottom ($z = 0$) and the top ($z = z_{\mathrm{max}}$) layers of the model and did, thus lead to a first compression. Afterwards the length of the original packing cell was reduced by the amount of the resulting compression of the polymer packing in z-direction followed by an adjustment of the z-coordinates of all atoms. Further equilibration was then achieved by stimulated annealing (cf. stages 5–7 of table 2). The whole 3-stage procedure was repeated as often as it was necessary to reach the measured or predicted density of the respective model. The resulting model geometries are described in table 3, which also

Table 2. Typical basic equilibration procedures. The individual stages lasted between 1 and 5 ps.

Stage of equilibration	*Status of p and T*	*Scaling factor for conformation energy terms in the force-field*	*Type of nonbonded interaction energy terms in the force-field*	*Scaling factor for atomic radii in nonbonded interaction energy terms*	*Integration time step in fs*
1	NVT 303K	0.001	Repulsive 4th order	0.5	0.05
2	NVT 303K	0.1	Repulsive 4th order	0.5	0.05
3	NVT 303K	0.1	Repulsive 4th order	2/3	0.05
4	NVT 303K	1	Repulsive 4th order	1	0.05
5	NVT 303 K	1	6–9 potential + Coulomb	1	0.2
6	NVT 600K	1	6–9 potential + Coulomb	1	0.5
7	NVT 303K	1	6–9 potential + Coulomb	1	1

contains respective data for the feed phase. This table also shows that for some of the polymers two independent models were constructed and simulated to get at least some idea about the reproducibility of these very time consuming simulations.

The computer time consuming MD simulations and subsequent data evaluation were mainly performed on the CRAY C916 of the Deutsches Klimarechenzentrum (DKRZ) in Hamburg and two Silicon Graphics Octane workstations. For all MD data production runs minimum image periodic boundary conditions with a (charge group based) cut-off distance of 12 Å for all non-bond interactions were applied. This value was about the longest possible cut-off radius to ensure minimum image periodic boundary conditions which demand that this value must be smaller than half the shortest dimension of the simulated packing model (lateral dimensions 24.5 Å). For neutral systems containing only partial charges, charge-group based cutoffs of this size have worked quite well also in foregoing studies [cf. e.g. 12–14].

The feed mixture models were also constructed using the amorphous cell module of the Accelrys software. There again a two-dimensionally (2D) periodic basic volume element was filled with the desired numbers of solvent molecules (table 3). The molecules were inserted in random sequence at random positions and with random orientations. After every insertion of a new molecule, the change of the system energy was calculated. Using these data the acceptance of the respective insertion was decided via the standard Metropolis criterion. Following the particle insertion procedure the subsequent equilibration was achieved according to table 4 with the last stage being performed for 200 ps.

After the complete refinement of each individual box the polymer and the feed boxes were layered onto each other along the *z*-axis and combined into a single simulation cell. Then periodic boundary conditions are applied in all three dimensions (3D-PBC) so that no energetic barriers force the atoms to remain in the given volume element. Thus, the simulation cell that contains on the average 6000 atoms is only one of an infinite number of periodically repeated simulation cells (figure 2). The number of included molecules and the boxlengths of the layered boxes for the different polymer–feed systems are listed in table 3. Due to the influence of the penalty surface potentials applied in the construction phase, immediately after the surface formation there is a small empty slit of a few Å thickness between the polymer and the feed phases (figure 2). To enable a smooth approach of polymer segments and solvent molecules into these slits and towards the real system density, about 50,000 steps of MD simulation were performed at 303 K with *NVT* ensembles at very small time steps of 0.05–0.1 fs. The MD production runs could then be performed with a time step of 1 fs as *NVT* ensembles for the overall simulation times and temperatures (mostly 303 K) given in table 3. The state of the model system, i.e. atomic positions and velocities, energy status, etc. of the respective simulation runs was saved every 500 fs in a history file. In total every model simulation was carried out for up to 8ns until either steady state was reached or the feed got depleted.

4. Results and discussion

In the case of the water/ethanol feed systems investigated earlier [12–14], the initial adsorptive behaviour of simulated interface models already gave a qualitative indication for the general separation trend to be expected during pervaporation. The interface simulations for the polysiloxanes for instance, in all cases reflected the expected preferential initial ethanol sorption. Already after 1 ns of a MD simulation the two feed components separated whereby the ethanol molecules accumulated at the respective polymer surfaces taking a favourite average orientation with the hydrophobic parts pointing in the direction of the polymer and the hydrophilic parts pointing in the direction of the water molecules. This was related with the fact that in pervaporation usually the sorption of feed molecules in the upstream top layer of a membrane is the most decisive step of the separation process. Therefore, also in the given case of the mentioned benzene/*n*-heptane mixture it was of interest to check possibilities for qualitative predictions of separation trends.

4.1 Initial adsorption

For illustrative purposes figure 3 shows the PMPhS-1 interface model just after the equilibration (0.1 ns MD simulation time), where the benzene molecules are still almost uniformly distributed in the feed phase.

Table 3. Basic data for the utilised polymer and feed models. The simulation time in the last column always is meant for the respective interface model (polymer–feed).

Model system	*Remarks*	*Number of atoms N*	*Length of z-axis for polymer model in Å (x,y=24.5 Å)*	*Length of z-axis for complete polymer–feed model in Å (x,y=24.5 Å)*	*Simulation temperature in K*	*Simulation time in ns*
Feed-1	Benzene/*n*-heptane (20:80)†	1448	26.3	n.a.	303	n.a.
Feed-2	Benzene/*n*-heptane (20:80)†	1448	28.5	n.a.	353	n.a.
PDMS	+Feed-1	2202	47.4	73.7	303	5.0
PMPhS-1	+Feed-1	2261	45.2	71.5	303	3.5
PMPhS-2	Continuation of PMPhS-1	2261	45.2	71.5	303	5.5
PMMA	+Feed-1	3000	46.7	73.0	303	3.0
PBMA	+Feed-1	2592	43.1	69.4	303	5.8
PNMA	+Feed-1	3100	52.7	79.0	303	4.0
PAMA	+Feed-1	3700	62.6	88.9	303	3.0
PtBMA-1	+Feed-1	3052	49.2	75.5	303	1.0
PtBMA-2	+Feed-1	3052	49.2	75.5	303	3.0
PMPhSMA-1	+Feed-1	3400	62.3	88.6	303	2.0
PMPhSMA-2	+Feed-2	3400	63.0	91.5	353	8.0

† Feed composition in wt%.

Table 4. Force-field scaling factors for the feed equilibration procedure. The integration time step was always 1 fs. The 6–9 nonbond pair interaction and the Coulomb potential of the pcff force-field were applied.

Stage of equilibration	*Scaling factor for conformation terms*	*Scaling factor for nonbond terms*
1	0.001	0.001
2	0.1	0.001
3	1	0.001
4	1	0.1
5	1	1

To get a quantitative description of the initial adsorption of feed molecules during the further course of the MD production run normalised density profiles for the polymer repeat units and the benzene and *n*-heptane molecules have been calculated in the following manner: A thin slice of a few Å thickness cut perpendicular to the *z*-axis of the model is moved through the model along the *z*-axis with a small step-width (a few tenth of an Å). In each slice the centroids of polymer repeat units and the respective centroids of benzene and *n*-heptane molecules are counted. The resulting density distribution functions are averaged over a large number of snapshots taken for the model geometry during the MD simulations. There, due to statistical problems the averaging can only be performed until a certain number of feed molecules has been absorbed in the polymer.

Figure 4 contains the respective density profiles for the PDMS-1 and PMPhS-1 models. It can clearly be recognised that in the case of PDMS the simulated initial adsorptive behaviour does not indicate any significant preferential permeation of either one feed component through this polymer. This is the same result as it was found experimentally [27].

Now the principle of similarity would suggest that the situation towards a more preferred benzene separation would improve if one of the methyl groups in each PDMS repeat unit would be replaced by a benzene group. That is exactly what is indicated in the upper part of figure 4 by the density profile for PMPhS, showing a significantly preferred benzene adsorption at the polymer surface.

Examples for the benzene and *n*-heptane adsorption on PMMA and some of its derivatives, however, are shown in figure 5.

It can be seen that from this point of view and in the series shown, the best separation effect would be expected for the basic glassy material PMMA. As mentioned before the reason for this behaviour is most likely an attractive interaction between the carbonyl groups of this polymer and the π-electrons of the benzene. There are also strong experimental indications of a preferred adsorption of benzene on PMMA that were, for example, observed in adsorption isotherm measurements [28]. PMMA is, however, a very brittle polymer which is not suited for the formation of thin membrane films needed to measure permeation effects. Therefore, several modifications (figure 1) were attempted not only to improve the

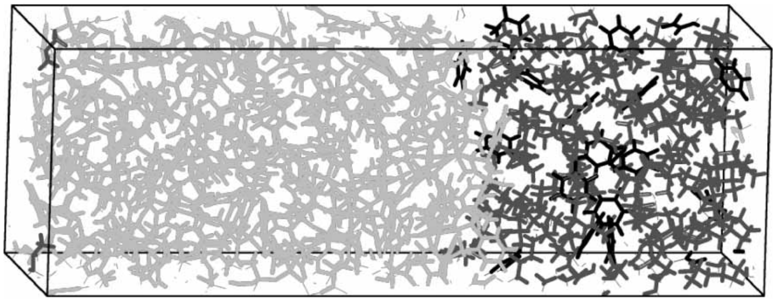

Figure 3. Representative view of the PMPhS-1 interface model after 0.1 ns MD simulation. Light grey = Polymer, dark grey = *n*-heptane, black = benzene. The long axis of the model is directed along the *z*-axis.

mechanical properties, but also to further increase the attractive interaction with benzene. But in fact those modifications obviously lead to a reduction of the carbonyl–benzene interaction, resulting in a decrease of benzene affinity. Most-likely large ester groups, such as benzyl (PBMA) and naphtyl (PNMA), "mask" the carbonyl groups of the respective polymers making them inaccessible for local interactions with the benzene molecules of the feed. Consequently, none of these modifications led to a more pronounced initial benzene adsorption in the interface simulations.

4.2 Initial absorption

Only in three cases, PMPhS, PMPhSMA and PtBMA the available simulation time of up to 8 ns was sufficient to allow a representative number of feed molecules to become completely absorbed in the polymer part of the respective model (cf. for the example of PMPhS figure 6).

In these cases it was possible to obtain an estimate for the solubility-related part of the separation factor of the respective polymer for benzene by averaging over a large number of available snapshots of the system taken during the MD simulation: $\alpha_{\text{benzene/heptane}}$ (equation (1)). There the averaging was performed from the simulation time step at which acceptable convergence of $\alpha_{\text{benzene/heptane}}$ could be found. For both polymers values of about 2 were obtained after sufficient simulation time. Thus, not even the investigated polymer (PMPhS) with the most preferred initial adsorption of benzene or the polymer (PtBMA) which showed the fastest initial diffusion (cf. below) did come close to the intended target for an industrial application, which is at about $\alpha_{\text{benzene/heptane}} = 10$.

Finally, some results concerning the model polymer PtBMA, which was expected to contain an increased amount of free volume (because of the bulky $C(CH_3)_3$ substituents) shall be discussed. As can be seen in figure 7 already after a relatively short simulation time penetrant molecules coming in from the left and right hand surface of the polymer phase almost meet each other in the middle of the polymer layer.

This is the fastest diffusion observed amongst the materials studied (the second fastest diffusion occurred in PMPhS-1, figure 6). In addition an effect related to

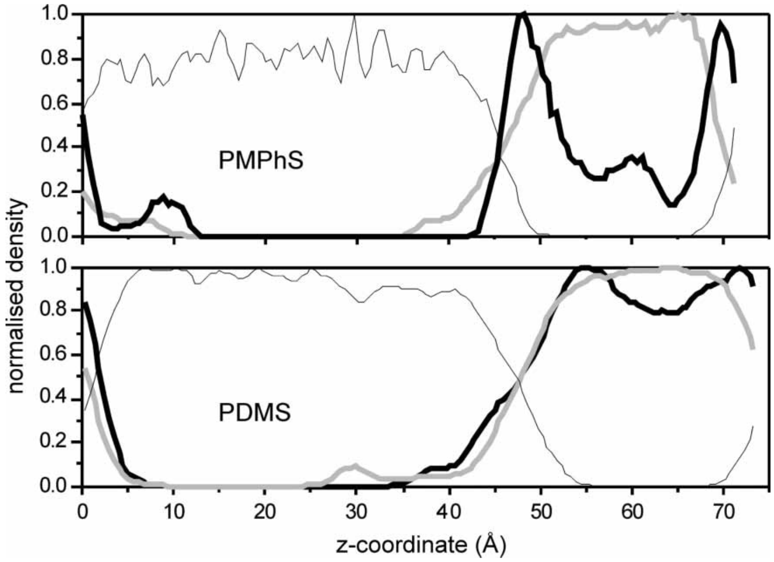

Figure 4. Normalised density profiles for polymer repeat units (thin grey line), benzene molecules (black line) and *n*-heptane molecules (thick grey line) as functions of the *z*-coordinate (in Å) of the PDMS and PMPhS-1 interface models (figure 3). PDMS was averaged over 5 ns while PMPhS-1 was averaged over 0.3 ns.

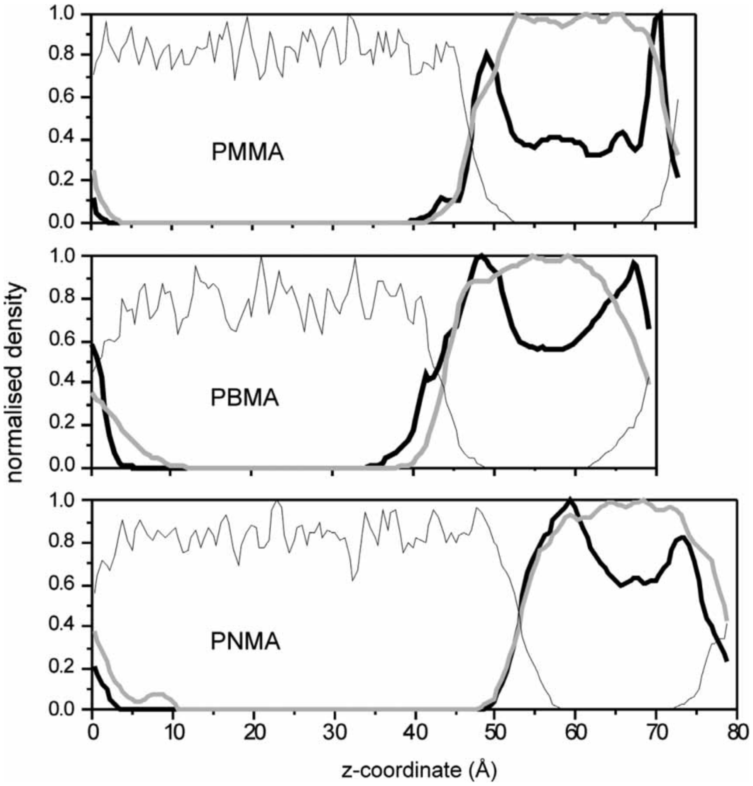

Figure 5. Normalised density profiles for polymer repeat units (thin grey line), benzene molecules (black line) and *n*-heptane molecules (thick grey line) as functions of the *z*-coordinate of the respective interface model (figure 3). PMMA averaged over 1 ns, PBMA and PBNA averaged over 2 ns.

the phenomenon, that in pervaporation membranes normally strong differences between pure and mixed feed transport behaviours (coupling of fluxes) exist, shall be mentioned. As confirmed by the following PtBMA model simulation results coupling of fluxes can strongly influence the separation behaviour. Due to the depletion of the feed from *n*-heptane and strong polymer swelling (preconditioning) the remaining excess component may be then absorbed preferentially. In about the first ns of MD simulation time the investigated PtBMA models are *n*-heptane selective (figure 7 (top)), i.e. in this time mostly *n*-heptane molecules are entering the polymer and cause local swelling effects. This swelling leads to laterally increased hole sizes which then permit also a larger number of benzene molecules to enter the model membrane. As result already after 2 ns the PtBMA is benzene selective (figure 7 (bottom)). Similar effects of one feed component helping the passage of another component are often found also in gas separation membranes particularly if one of the feed constituents is CO_2 [29]. In order to compensate such effects in the simulations the depleted feed has to be “refilled” by substitution of the excess component with the missing component.

4.3 Diffusion mechanism

In several examples differences in the diffusion behaviour between the conformationally stiff benzene and the conformationally flexible *n*-heptane could be

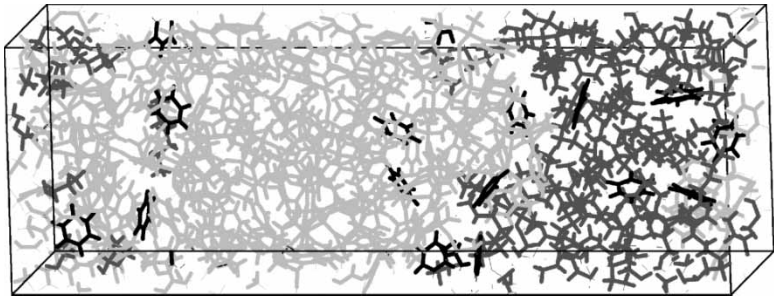

Figure 6. Representative view of the PMPhS-1 interface model after 5.5 ns MD simulation. Light grey = Polymer, dark grey = *n*-heptane, black = benzene. The long axis of the model is directed along the *z*-axis.

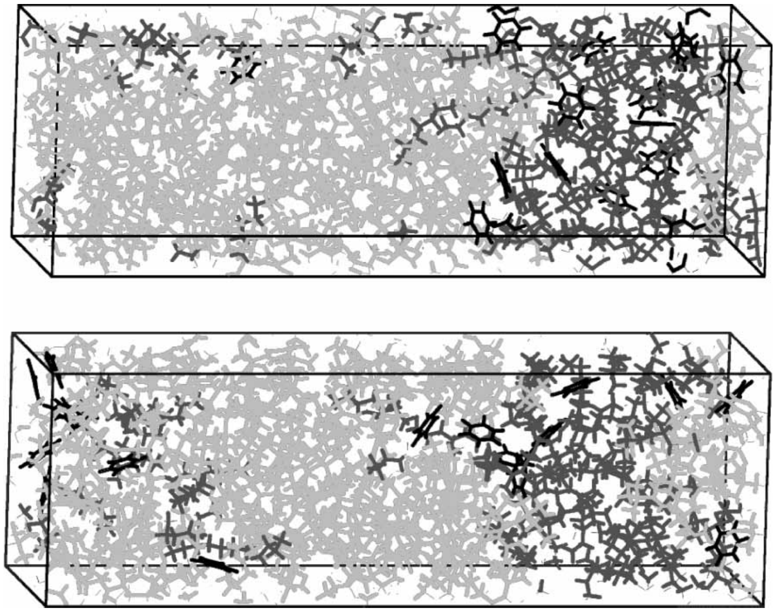

Figure 7. Representative view of the PtBMA-2 interface model after 1 ns (top) and after 2 ns (bottom) MD simulation. Light grey = Polymer, dark grey = *n*-heptane, black = benzene. The long axis of the model is directed along the *z*-axis.

observed. These effects could be best seen for the two polymer models with the fastest diffusion of penetrants (PMPhS-2 and PtBMA-2). Here, the conformationally flexible *n*-heptane molecules follow preferentially the course of diffusion channels with a basically continuous diffusion along the voids, while the rigid benzene molecules rather remain in suited voids for up to several hundred picoseconds. Whenever then channels between two adjacent voids are opening jump events become possible, resulting in a “jump-like” diffusion mechanism of benzene similar to the case of small molecules (e.g. H_2, N_2, O_2) in gas separation membranes [2]. This behaviour can be well recognised from graphic displays of a travelled distance $R(t)$ of a molecule as function of simulation time t. Figure 8 shows the typical movements of each a representative benzene and *n*-heptane molecule in glassy PtBMA.

Using the simulation data it is also possible to visualise the repetition-like mechanism of individual *n*-heptane molecules. Figure 9 shows an example where an *n*-heptane

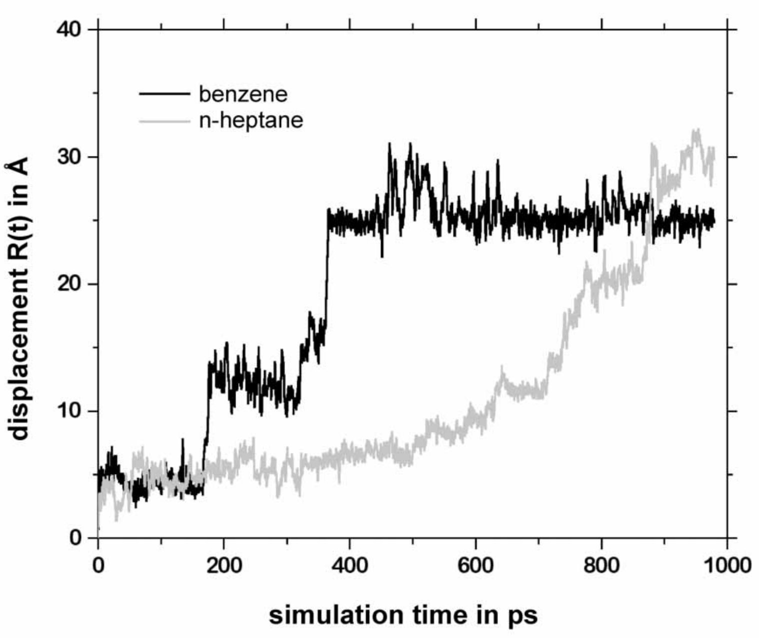

Figure 8. Displacement $R(t)$ vs simulation time t for a typical benzene and a typical *n*-heptane molecule in PtBMA.

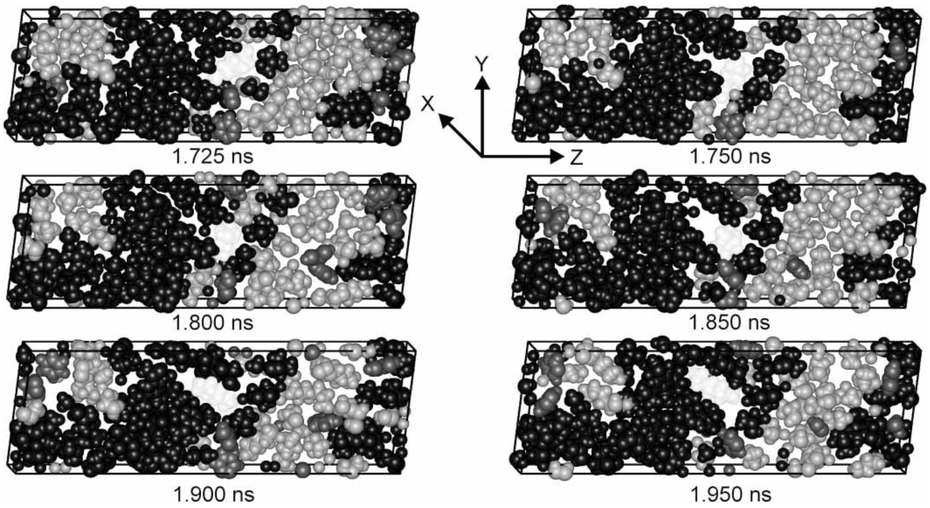

Figure 9. Slithering move of a n-heptane molecule in PtBMA shown in a 5 Å thick slice cut out of the PtBMA-2 model perpendicular to the x-axis direction. Black = Polymer, light grey = n-heptane molecule of interest, grey = other n-heptane and benzene molecules.

molecule (white colour) is progressing by a transformation from a relatively extended state at a simulation time of 1.725 ns via a highly coiled state in the area of 1.800 ns to again an energetically favourable, extended configuration at 1.900 ns.

5. Summary

The theoretical approach towards the separation problem of an organic/organic feed mixture of 20 wt% benzene and 80 wt% n-heptane with dense amorphous polymer membranes was investigated utilising molecular modelling techniques. It could be demonstrated that MD simulations of polymer–feed interface models can reproduce at least qualitatively important experimental results from related membrane pervaporation processes. For this purpose mainly the initial adsorption of feed molecules at the polymer surface and the subsequent initial stages of absorption were considered. These models are, therefore, suited to obtain a better insight in the mechanisms of pervaporation on atomistic length scale. For example it was found that both size and electrostatic properties of ester groups as well as void size and distribution in the polymer strongly influence the benzene affinity of PMMA derivatives.

However, all model polymers which were studied as membranes materials for the above mentioned separation problem did not show a trend to a sufficient selectivity for industrial applications in the MD simulations. Thus, afterwards laboratory efforts for chemical synthesis, membrane formation and characterisation of a number of these materials could be avoided.

In addition, the knowledge about the underlying diffusion mechanism has been improved. It could be for instance shown that the rigid benzene penetrants diffuse in a jump-like manner between adjacent holes of the respective polymer matrix while the flexible n-heptane molecules follow a more continuous diffusion style.

Acknowledgements

We thank Dr Schwarz (GKSS) and Regine Apostel (GKSS) for the pervaporation measurements on PDMS films and Christine Dannenberg (Technical University of Berlin) for the measured density values. We would like to acknowledge that parts of the work were supported by the European Commission "Growth" Program, "PERMOD—Molecular modelling for the competitive molecular design of polymer materials with controlled permeability properties.", Contract #G5RD-CT-2000-200.

References

[1] F. Müller-Plathe. Permeation of polymers—A computational approach. *Acta Polym.*, **45**, 259 (1994).
[2] D. Hofmann, L. Fritz, J. Ulbrich, C. Schepers, M. Böhning. Detailed-atomistic molecular modelling of small molecule diffusion and solution processes in polymeric membrane materials. *Macromol. Theory Simul.*, **9**, 293 (2000).
[3] Y. Tamai, H. Tanaka, K. Nakanishi. Molecular simulation of permeation of small penetrants through membranes. 1. Diffusion coefficients. *Macromolecules*, **27**, 4498 (1994).
[4] Y. Tamai, H. Tanaka, K. Nakanishi. Molecular simulation of permeation of small penetrants through membranes. 1. Solubilities. *Macromolecules*, **28**, 2544 (1995).
[5] F. Müller-Plathe. Diffusion of water in swollen poly(vinyl alcohol) membranes studied by molecular dynamics simulation. *J. Membr. Sci.*, **141**, 147 (1998).
[6] M. Wesslein, A. Heintz, R.N. Lichtenthaler. Pervaporation of liquid mixtures through poly(vinyl alcohol) (PVA)-membranes. I. Study of water containing binary systems with complete and partial miscibility. *J. Membr. Sci.*, **51**, 169 (1990).
[7] R.Y.M. Huang (Ed.). *Pervaporation Membrane Separation Processes*, Elsevier Science, Amsterdam (1991).
[8] J.M. Watson, G.S. Zhang, P.A. Payne. The diffusion mechanism in silicon rubber. *J. Membr. Sci.*, **73**, 55 (1992).
[9] T.M. Aminabhavi, R.S. Khinnavar, S.B. Harpogoppad, Q.T. Nguyen, K.C. Hansen. Pervaporation Separation of organic–aqueous and organic–organic binary mixtures. *J. Membr. Sci. Rev. Macromol. Chem. Phys.*, **C34**(2), 139 (1994).
[10] J.M. Watson, P.A. Payne. A study of organic compound pervaporation through silicone rubber. *J. Membr. Sci.*, **49**, 171 (1990).
[11] M. Mulder. *Basic Principles of Membrane Technology*, Kluwer Academic Publishers, Dordrecht (1991).

[12] L. Fritz, D. Hofmann. Molecular dynamics simulations of the transport of water–ethanol mixtures through polydimethylsiloxane membranes. *Polymer*, **38**, 1035 (1997).

[13] L. Fritz, D. Hofmann. Behaviour of water–ethanol mixtures in the interfacial region of different polysiloxane membranes—a molecular dynamics simulation study. *Polymer*, **39**, 2531 (1998).

[14] D. Hofmann, L. Fritz, D. Paul. Molecular modeling of pervaporation separation of binary mixtures with polymeric membranes. *J. Membr. Sci.*, **144**, 145 (1998).

[15] G. Malsch (GKSS Research Center). Personal communication.

[16] K. Inui, H. Okamura, T. Miyata, T. Uragami. Permeation and separation of benzene/cyclohexane mixtures through cross-linked poly(alkyl methacrylate) membranes. *J. Membr. Sci.*, **132**, 193 (1997).

[17] K. Inui, T. Noguchi, T. Miyata, T. Uragami. Pervaporation characteristics of methyl methacrylate–methacrylic acid copolymer membranes ionically crosslinked with metal ions for a benzene/cyclohexane mixture. *J. Appl. Polym. Sci.*, **71**, 233 (1999).

[18] K. Kusakabe, S. Yoneshige, S. Morooka. Separation of benzene/cyclohexane mixtures using polyurethane–silica hybrid membranes. *J. Membr. Sci.*, **149**, 29 (1998).

[19] Molecular Simulations Inc., (1999), Computational results obtained using software programs from Molecular Simulations Inc. of San Diego-molecular mechanics calculations from Discover (Version 4.0.0p+) and graphical display using InsightII, (1999).

[20] H. Sun, S.J. Mumby, J.R. Maple, A.T. Hagler. An *ab initio* CFF93 all-atom force field for polycarbonates. *J. Am. Chem. Soc.*, **116**, 2978 (1994).

[21] Polymer User Guide Synthia Section, *Version 400p+*, Molecular Simulations Inc., San Diego (1999).

[22] J. Bicerano. *Prediction of Polymer Properties*, Marcel Dekker, New York (1993).

[23] D.N. Theodorou, U.W. Suter. Detailed molecular structure of a vinyl polymer glass. *Macromolecules*, **18**, 1467 (1985).

[24] D.N. Theodorou, U.W. Suter. Atomistic modeling of mechanical properties of polymeric glass. *Macromolecules*, **19**, 139 (1986).

[25] ABCR-Catalogue 1994/95, *Research Chemicals*, ABCR GmbH and Co., Karlsruhe (1994).

[26] C. Dannenberg (Technical University of Berlin). Personal communication.

[27] H.H. Schwarz (GKSS Research Center). Personal communication.

[28] A. Wenzel, H. Yanagishita, D. Kitamoto, A. Endo, K. Haraya, T. Nakane, N. Hanai, H. Matsuda, N. Koura, H. Kamusewitz, D. Paul. Effects of preparation condition of photoinduced graft filling-polymerized membranes on pervaporation performance. *J. Membr. Sci.*, **179**, 69 (2000).

[29] C. Staudt-Bickl, W.J. Koros. Improvement of CO_2/CH_4 separation characteristics of polyimides by chemical crosslinking. *J. Membr. Sci.*, **155**, 145 (1999).